

# Supporting information for: Evaluating Thermal Corrections for Adsorption Processes at the Metal/Gas Interface

Romain Réocreux,<sup>†</sup> Carine Michel,<sup>†</sup> Paul Fleurat-Lessard,<sup>‡</sup> Philippe Sautet,<sup>¶,§</sup> and  
Stephan N. Steinmann<sup>\*,†</sup>

<sup>†</sup>*Univ Lyon, Ecole Normale Supérieure de Lyon, CNRS Université Lyon 1, Laboratoire de  
Chimie UMR 5182, 46 allée d'Italie, F-69364, LYON, France*

<sup>‡</sup>*Université de Bourgogne Franche-Comté(UBFC), Institut de Chimie Moléculaire de  
l'Université de Bourgogne (ICMUB), UMR CNRS 6302, 9 avenue Alain Savary 21078 Dijon,  
France*

<sup>¶</sup>*Department of Chemical and Biomolecular Engineering, University of California, Los  
Angeles, Los Angeles, CA 90095, USA*

<sup>§</sup>*Department of Chemistry and Biochemistry, University of California, Los Angeles, Los  
Angeles, CA 90095, USA*

E-mail: [stephan.steinmann@ens-lyon.fr](mailto:stephan.steinmann@ens-lyon.fr)

## Contents

<b>1</b>	<b>Computational Details for Thermodynamic Integration</b>	<b>S2</b>
1.1	Integration procedure . . . . .	S3

1.2	Thermodynamics and kinetics of surface/gas events . . . . .	S3
<b>2</b>	<b>Statistical mechanics for the gas-phase and adsorbates</b>	<b>S6</b>
2.1	Translation . . . . .	S6
2.2	Rotation . . . . .	S7
<b>3</b>	<b>Thermostat</b>	<b>S7</b>
<b>4</b>	<b>Additional Tables</b>	<b>S7</b>
<b>5</b>	<b>Geometric features of CO<sub>2</sub> at the transition state</b>	<b>S11</b>
<b>6</b>	<b>Geometric features of CO<sub>2</sub> chemisorption minimum</b>	<b>S11</b>
	<b>References</b>	<b>S12</b>

# 1 Computational Details for Thermodynamic Integration

We chose the average carbon – metal surface distance as the reaction coordinate for desorption of all molecules, except for CO, where the centre of mass is more appropriate as it prevents the necessity to discriminate between parallel and perpendicular adsorption modes, a feature of particular significance at short adsorbate to metal distances.

The average Pt – C surface distance is not the perfect reaction coordinate for the  $\eta^6$  to  $\eta^3$  adsorption mode of C<sub>6</sub>Cl<sub>6</sub>. Nevertheless, the free energy profile converged reasonably well within  $\sim 15$  ps of dynamics for the points around the transition state.

In TI, the free energy is obtained as the integral of the free energy gradient along the reaction coordinate  $\xi$ . We have determined the free energy gradient and its statistical uncertainty according to the blocking algorithm<sup>S1</sup> as implemented in the pyblock module.<sup>S2</sup> The convergence of the simulation is determined as follows: After an equilibration time of at 1-3 ps, simulations of 1 ps are added until the gradient does not change by more than 0.02

eV/Å, using at least 3 ps.

Altogether, we total 145 ps for CO<sub>2</sub> and 150 ps for formic acid adsorption energy profiles, with a computational cost of roughly 15 kCPUh. For CO adsorption, we have roughly 160 ps for 300 K and 100 ps for 600 K, totaling to a combined computational cost of 70 kCPUh. Phenol and hexachlorobenzene adsorption required 85 ps and 170 ps, respectively, corresponding to a computational cost of 45 kCPUh and 95 kCPUh. It is worth noting that one advantage of TI is that each point is independent of the others, so that all constrained molecular dynamic simulations can be launched in parallel.

## 1.1 Integration procedure

The integration of the gradients was performed using the trapezoid method. In order to estimate the propagation of errors during integration, we first determined, for each simulation  $i$ , the standard deviation  $\sigma_i$  of the  $n_i$  gradients  $g_j$  according to the blocking algorithm of Flyvbjerg and Petersen.<sup>S1</sup>

The cumulative standard deviation  $S_i$  on the overall integration starting at the largest reaction coordinate  $\xi$ , indexed as 1, is obtained as:

$$S_i = \sqrt{\sum_{k>1}^i (\xi_k - \xi_{k-1})^2 \cdot \sigma_k^2} \tag{1}$$

The curves of  $\Delta F_N \pm 2S_N$  give a 95 % confidence interval for the integration and therefore assesses its precision.

## 1.2 Thermodynamics and kinetics of surface/gas events

Let us consider the species  $S$  in gas-phase at a pressure  $p$  (and standard pressure  $p^0$ ) in equilibrium with its adsorbed state  $S^*$  at a surface coverage  $\theta$  (and a standard coverage  $\theta^0$ ). Following the works by Campbell and coworkers<sup>S3</sup> and the earlier formalism by Pitt et al.<sup>S4</sup>

the desorption rate constant  $k_{des}$  is written as:

$$k_{des} = \kappa \frac{k_B T}{h} \frac{q^\ddagger/A}{q_{ads}/A} \exp\left(-\frac{\Delta H^\ddagger}{k_B T}\right) \quad (2)$$

where  $\kappa$  is the transmission coefficient,  $q_{ads}$  is the vibrational partition function on the surface and  $q^\ddagger$  is the corresponding partition function of the transition state for desorption,  $\Delta H^\ddagger$  is the activation enthalpy for desorption, the  $k_B$  is Boltzmann's and  $h$  Planck's constant. Here both,  $q$  and  $q^\ddagger$  are referring to a two dimensional system, which is indicated by the division by the surface area  $A$  considered.

The second crucial quantity is the equilibrium constant for desorption,  $K_{eq}$ , the ratio between  $a_{S_{gas}}$ , the activity of the species  $S$  in gas phase and  $a_{S_{ads}}$ , the one of the adsorbed species  $S^*$ .

$$K_{eq} = \frac{a_{S_{gas}}}{a_{S_{ads}}} \quad (3)$$

$$= \frac{p/p^0}{\theta/\theta^0} \quad (4)$$

$$= \frac{p}{\theta} \cdot \frac{\theta^0}{p^0} \quad (5)$$

$$= \frac{q_{gas}/V}{q_{ads}/A} \cdot \frac{N_{ads}^0/A^0}{N_g^0/V^0} e^{\frac{-\Delta H}{k_B T}} \quad (6)$$

$$= \frac{q_{gas}/V}{q_{ads}/A} \cdot \frac{V^0}{N_g^0} \frac{N_{ads}^0}{A^0} e^{\frac{-\Delta H}{k_B T}} \quad (7)$$

$$= \frac{q_{gas}/V}{q_{ads}/A} \cdot \frac{k_B T}{p^0} e^{1/3} \left(\frac{k_B T}{p^0}\right)^{-2/3} e^{\frac{-\Delta H}{k_B T}} \quad (8)$$

$$= \frac{q_{gas}/V}{q_{ads}/A} \cdot \left(\frac{k_B T}{p^0}\right)^{1/3} e^{1/3} e^{\frac{-\Delta H}{k_B T}} \quad (9)$$

where we have used  $q_{gas}$  for the vibrational translational and rotational partition function of the gas-phase,  $V$  and  $A$  are the volume and surface area, respectively,  $N$  is the number of molecules,  $\Delta H$  is the reaction enthalpy for desorption and  $R$  the ideal gas-constant.  $e^{1/3} \left(\frac{k_B T}{p^0}\right)^{-2/3}$  is the factor taking care of the standard state conversion from the gas phase

to the surface. It has the units of a length (volume to surface ratio,  $L$ ) and is taken from the consistent definition of standard states for adsorbates and the gas-phase as introduced by Campbell and co-workers.<sup>S3</sup>

Since the desorption equilibrium constant can also be written as

$$K_{eq} = \frac{k_{des}}{k_{ads}} \tag{10}$$

where  $k_{ads}$  is the rate constant for adsorption, we can write

$$k_{ads} = \kappa' \frac{k_B T}{h} \frac{q^\ddagger/A}{q_{gas}/V} \exp\left(-\frac{\Delta H^\ddagger'}{k_B T}\right) \left(\frac{k_B T}{p^0}\right)^{-1/3} e^{-1/3} \tag{11}$$

where primed quantities refer to the reverse sense compared to equation 2.

Equation 2 is straight forward to compare to the results from thermodynamic integrations, as no dimensionality change occurs between the transition state and the adsorbed state. Furthermore, in a system without an energy barrier for desorption, the transition state is formally at infinite separation from the surface, but still restricted to the surface area  $A$  of the system. The situation is more delicate for Equation 11: In this case, we need to take into account the volume of the gas phase ( $V$ ) and the surface area ( $A$ ) to which the transition state is constrained. Since in our periodic slab model the molecule can never “escape” the transition state (at infinite separation) and is always restricted to move on top of the surface, we cannot use Equation 11 for comparison with the AIMD results. This situation differs from the case where a nano-particle would be used as the surface model instead of the slab: In this case, upon desorption, the molecule would be able to explore three dimensional space and AIMD would be comparable to the three “standard” three dimensional treatment applied for bi-molecular reactions. Note, that even in general, Eq. 11 requires the knowledge of the surface to volume ratio of the reactor/vessel used, while Eq. 2 is an intrinsic quantity of the surface.

## 2 Statistical mechanics for the gas-phase and adsorbates

### 2.1 Translation

The partition function  $q_{trans}$  for molecules in the (ideal) gas-phase is given by:

$$q_{trans}^{gas} = \frac{A \times \ell}{\Lambda^3} \quad \text{with} \quad \Lambda = \frac{h}{\sqrt{8\pi m k_B T}} \quad (12)$$

where  $A$  is the area and  $\ell$  the length of the volume available to the molecule.  $h$  and  $k_B$  are Planck's and Boltzmann's constant, respectively, while  $T$  is the temperature in Kelvin and  $m$  the mass of the molecule.

If the translation is restricted to two dimensions, i.e., *sliding* of an ideal 2D gas, as it is the case for the desorption transition state at infinite separation, the translational partition function is reduced to:

$$q_{trans}^{sliding} = \frac{A}{\Lambda^2} \quad \text{with} \quad \Lambda = \frac{h}{\sqrt{8\pi m k_B T}} \quad (13)$$

where  $A$  is the area of the solid surface.

For our surfaces, the translational entropy at one point in the free energy profile can, in principle, be determined based on the principle root mean square fluctuation  $\sigma$  of the center of the mass of the molecule during the AIMD.<sup>S5</sup>

$$S(\xi)^{trans} = R \ln \left( \frac{24\pi e m k_B T}{h^2} \sigma_q(\xi) \sigma_{q'}(\xi) \right) \quad (14)$$

with  $e$  Euler's number,  $m$  the molecular mass and  $\sigma_q(\xi)$  is the principle root mean square fluctuation for the center of mass of the molecule at  $\xi$  in the direction  $q$  perpendicular to  $\xi$ .

The computation of  $\sigma$  requires about 10 ps to be converged for a freely translating gas around 300 K and the convergence is slowed down by the stochastic thermostat. According to our tests, for CO<sub>2</sub> in the middle of the simulation box, it takes more than 30 ps to fully

converge  $\sigma$ .

## 2.2 Rotation

In the rigid rotator approximation, the rotational partition function ( $q_{rot}$ ) of a molecule in gas phase reads:

$$q_{rot}^{gas} = \frac{\sqrt{\pi}}{\sigma} \times \sqrt{\frac{(k_B T)^3}{ABC}} \quad (15)$$

where  $\sigma$  is the symmetry number and  $A, B, C$  the rotational constants.

## 3 Thermostat

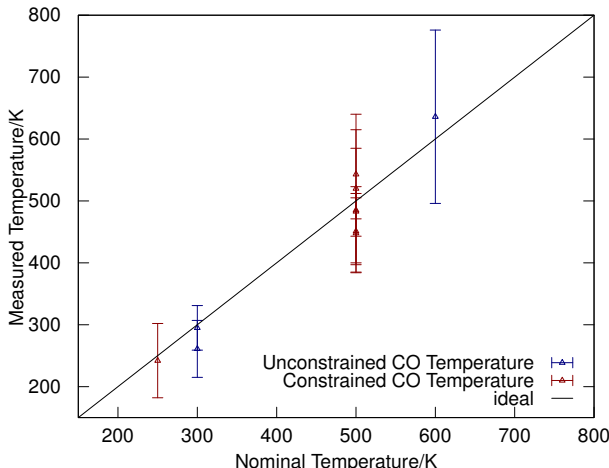


Figure S1: The measured temperature as a function of the nominal temperature for selected simulations of CO. For unconstrained dynamics, the nominal temperature is identical to the temperature of the thermostat, while for constrained dynamics, one degree of freedom is lost. The error bars have been determined via the blocking algorithm.<sup>S1</sup> Several simulations are run, either changing the initial configuration or velocities, or using a Lowe-Anderson<sup>S6</sup> instead of the pure Anderson thermostat.

## 4 Additional Tables

To estimate the effect of slab thickness on the convergence of free energies we performed further calculations for PhOT and C<sub>6</sub>Cl<sub>6</sub> on a 4-layer slab. The structures were relaxed

Table S1: List of the three *vertical thermal corrections* studied in the present work. For the translational modes ( $\Delta S_{trans}$ ), we use the Sackur-Tetrode (ST) formula for a 2D ideal gas. The harmonic oscillator (HO) is used for vibrations and the rigid rotor (RR) for gas-phase rotations.

Name $\Delta S_{trans}$	Procedure <i>Adsorbates</i> : No free energy corrections <i>Gas phase</i> : Translational entropy of a 2D ideal gas corresponding to the desorption transition state
RRHO	<i>Adsorbates</i> : HO for all modes <i>Gas phase</i> : HO for all modes but rotations (RR) and translations (ST)
cut-off <sup>S7</sup>	<i>Adsorbates</i> : HO for all modes above the cut-off value (100 cm <sup>-1</sup> ) <i>Gas phase</i> : same as RRHO
renormalization <sup>S8</sup>	<i>Adsorbates</i> : HO for all modes after replacing frequencies below the cut-off value by the cut-off value (100 cm <sup>-1</sup> ) <i>Gas phase</i> : same as RRHO

Table S2: Vertical corrections (in eV) for the various adsorbates. A: Area of the unit cell; ZPE: zero point energy;  $T\Delta S_{trans}$  is the difference with respect to the desorption transition state at infinity assuming an ideal 2D gas for the TS and the complete loss of this entropy upon adsorption; RRHO: Rigid rotor harmonic oscillator approximation; Cut-off: Like RRHO, frequencies below 100 cm<sup>-1</sup> are neglected; Renorm: Like RRHO, frequencies below 100 cm<sup>-1</sup> are reset to 100 cm<sup>-1</sup>; TI: thermodynamic integration, it refers to the free energy correction obtained by subtracting the 0 K adsorption energy from the TI free energy minimum. The mean absolute deviation is given for the vertical corrections and the average statistical uncertainty for TI and is therefore highlighted in italics.

	A (in Å <sup>2</sup> )	$\Delta ZPE$	$T\Delta S_{trans}$	RRHO	Cutoff	Renorm	TI
CO (220±20K)	25.3	0.06	0.15±0.02	0.26±0.03	0.23±0.02	0.25±0.02	0.25±0.08
CO (480±50K)	25.3	0.06	0.35±0.04	0.60±0.07	0.51±0.06	0.56±0.06	0.38±0.08
CO <sub>2</sub> (250K)	61.4	0.00	0.20	0.25	0.29	0.27	0.24
CO <sub>2</sub> TS (250K)	61.4	-0.03	0.20	0.22	0.30	0.25	0.12
HCOOH (270K)	61.4	0.01	0.22	0.34	0.42	0.36	0.22
C <sub>6</sub> H <sub>6</sub> (300K)	110.3	0.02	0.27	0.57	0.45	0.50	0.51
C <sub>6</sub> H <sub>5</sub> OH (300K)	110.3	0.00	0.28	0.60	0.54	0.56	0.53
C <sub>6</sub> Cl <sub>6</sub> $\eta^6$ (300K)	110.3	-0.04	0.30	0.56	0.65	0.57	0.56
C <sub>6</sub> Cl <sub>6</sub> TS $\eta^{6\rightarrow3}$ (300K)	110.3	-0.06	0.30	0.56	0.64	0.57	0.37
C <sub>6</sub> Cl <sub>6</sub> $\eta^3$ (300K)	110.3	-0.04	0.30	0.56	0.65	0.57	0.52
C <sub>6</sub> Cl <sub>6</sub> TS $\eta^{3\rightarrow0}$ (300K)	110.3	-0.02	0.30	0.51	0.68	0.53	0.40
C <sub>6</sub> Cl <sub>6</sub> $\eta^0$ (300K)	110.3	0.03	0.30	0.42	0.71	0.51	0.39
<b>MAD</b>	NA	NA	0.12	0.08	0.15	0.09	<i>0.18</i>

Table S3: Influence slab thickness on the energetics and vertical corrections.

state	4 layers				deviation from 3 layers			
	E(0K)	RRHO	Cutoff	Renorm	$\Delta_E$	$\Delta_{RRHO}$	$\Delta_{cutoff}$	$\Delta_{renorm}$
$C_6H_5OT$	-1.72	0.36	0.70	0.50	0.58	-0.05	0.00	0.00
$C_6Cl_6\eta^6$ (300K)	-0.98	0.51	0.61	0.56	0.49	-0.05	-0.04	-0.01
$C_6Cl_6$ TS $\eta^{6\rightarrow3}$ (300K)	-0.55	0.52	0.60	0.55	0.67	-0.04	-0.04	-0.01
$C_6Cl_6\eta^3$ (300K)	-1.12	0.49	0.64	0.54	0.52	-0.08	-0.01	-0.03
$C_6Cl_6$ TS $\eta^{3\rightarrow0}$ (300K)	-0.58	0.38	0.70	0.52	0.64	-0.13	0.01	-0.01
$C_6Cl_6\eta^0$ (300K)	-1.49	0.36	0.70	0.50	-0.02	-0.05	0.00	0.00

keeping the atoms of the bottom two layers at their bulk position. In order to be consistent with the previous estimation of the free energy (and limit the number of ill-defined phonons), we then performed a vibrational analysis using a finite difference algorithm on the top-most layer of the slab and the adsorbate only. The influence of the fourth layer on the energy is large for adsorbates chemically bound to the surface: all structures are less stable by 0.5-0.6 eV (see Table S3). It is expected as the electrons of the metal are confined in a very narrow slab and the electronic properties of the metal are not converged. For the physisorbed state of  $C_6Cl_6$ , the energy relative to gas phase is not impacted. More interestingly, the deviations on the vertical corrections are essentially negative, probably because of the loser interaction of the adsorbates with the surface as already evidenced with the adsorption energies. RRHO show the large, but still moderate, deviations (up to -0.13 eV) whereas the Cutoff and Renormalisation methods are more robust in terms of convergence with respect to slab thickness (see Table S3).

The faster convergence of the vertical corrections over energies opens the possibility of doing a very accurate calculation for the estimation of the energy and then use thinner slabs for the more expensive vibrational analysis.

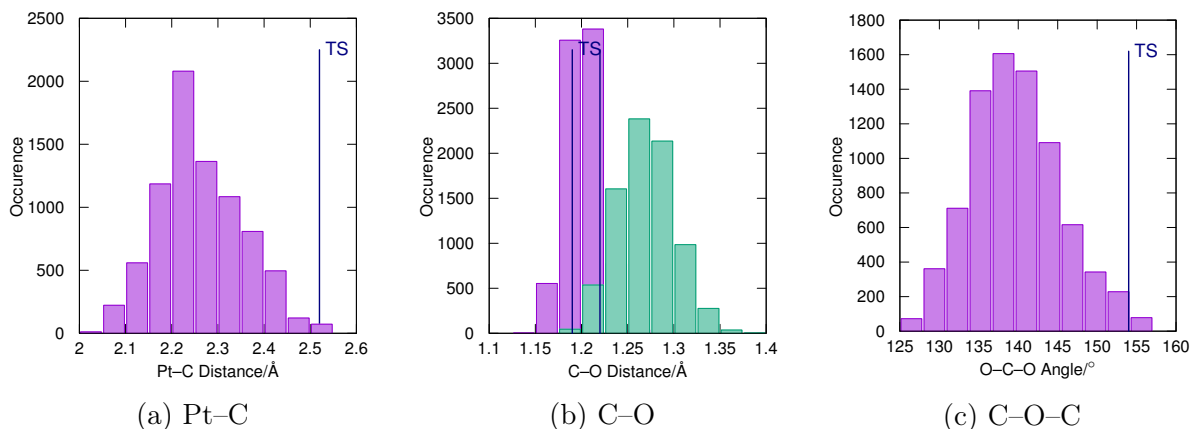


Figure S2: Distributions of key geometric features for  $\text{CO}_2$  close to the adsorption transition state (2.34 Å above the Pt(111) surface) over the last 8 ps of dynamics.

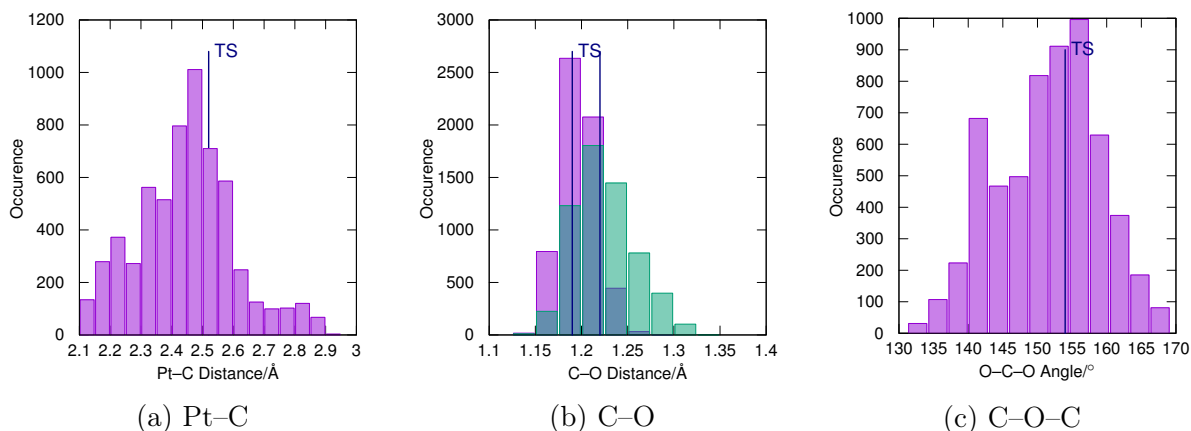


Figure S3: Distributions of key geometric features for  $\text{CO}_2$  close to the TI adsorption transition state (2.36 Å above the Pt(111) surface) over the last 6 ps of dynamics.

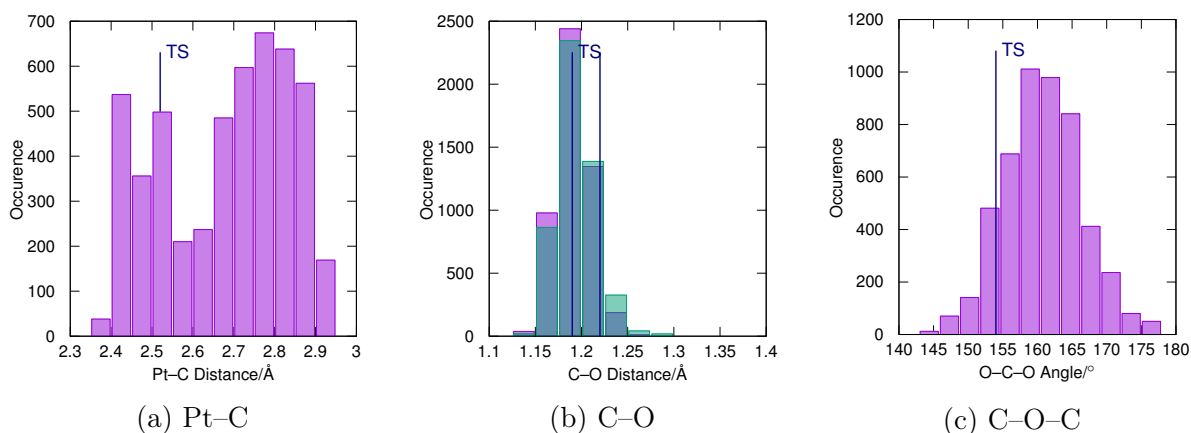


Figure S4: Distributions of key geometric features for  $\text{CO}_2$  at its static adsorption transition state (2.39 Å above the Pt(111) surface) over the last 5 ps of dynamics.

## 5 Geometric features of CO<sub>2</sub> at the transition state

## 6 Geometric features of CO<sub>2</sub> chemisorption minimum

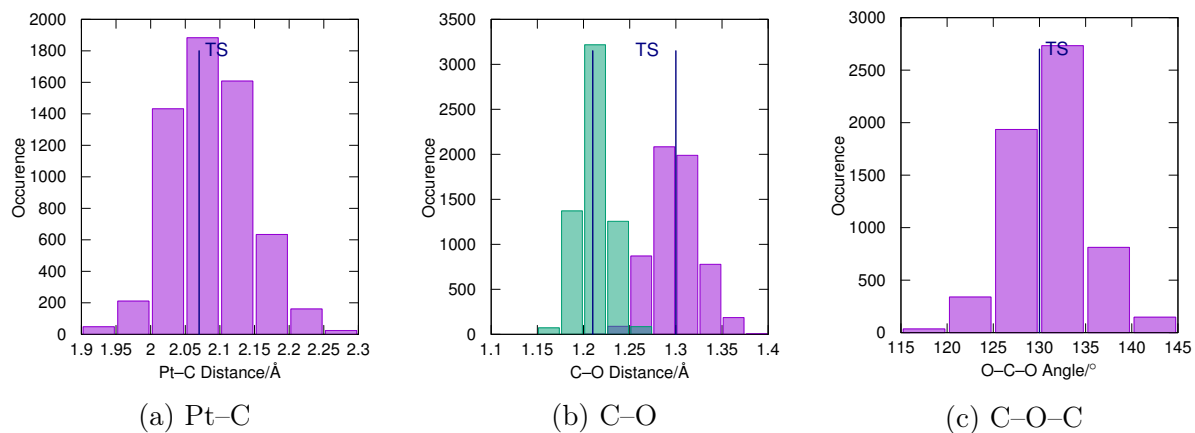


Figure S5: Distributions of key geometric features for CO<sub>2</sub> close to chemisorption minimum (2.04 Å above the Pt(111) surface) over the last 6 ps of dynamics.

## References

- (S1) Flyvbjerg, H.; Petersen, H. G. Error Estimates on Averages of Correlated Data. *J. Chem. Phys.* **1989**, *91*, 461–466.
- (S2) Spencer, J. Pyblock, see <https://github.com/jsspencer/pyblock/blob/master/docs/index.rst>. (accessed October 28, 2019).
- (S3) Campbell, C. T.; Sprowl, L. H.; Arnadottir, L. Equilibrium Constants and Rate Constants for Adsorbates: Two-Dimensional (2D) Ideal Gas, 2D Ideal Lattice Gas, and Ideal Hindered Translator Models. *J. Phys. Chem. C* **2016**, *120*, 10283–10297.
- (S4) Pitt, I. G.; Gilbert, R. G.; Ryan, K. R. Application of Transition-State Theory to Gas-Surface Reactions: Barrierless Adsorption on Clean Surfaces. *J. Phys. Chem.* **1994**, *98*, 13001–13010.
- (S5) Carlsson, J.; Aqvist, J. Absolute and Relative Entropies from Computer Simulation with Applications to Ligand Binding. *J. Phys. Chem. B* **2005**, *109*, 6448–6456.
- (S6) Koopman, E. A.; Lowe, C. P. Advantages of a Lowe-Andersen Thermostat in Molecular Dynamics Simulations. *J. Chem. Phys.* **2006**, *124*, 204103.
- (S7) Steinmann, S. N.; Michel, C.; Schwiedernoch, R.; Filhol, J.-S.; Sautet, P. Modeling the HCOOH/CO<sub>2</sub> Electrocatalytic Reaction: When Details Are Key. *ChemPhysChem* **2015**, *16*, 2307–2311.
- (S8) Zhao, Y.; Truhlar, D. G. Computational Characterization and Modeling of Buckyball Tweezers: Density Functional Study of Concave-Convex  $\pi \cdots \pi$  Interactions. *Phys. Chem. Chem. Phys.* **2008**, *10*, 2813–2818.